

Mechanism of IS200/IS605 Family DNA Transposases: Activation and Transposon-Directed Target Site Selection

Orsolya Barabas,¹ Donald R. Ronning,^{1,3,4} Catherine Guynet,^{2,4} Alison Burgess Hickman,¹ Bao Ton-Hoang,² Michael Chandler,² and Fred Dyda^{1,*}

¹Laboratory of Molecular Biology, National Institute of Diabetes, Digestive, and Kidney Diseases, National Institutes of Health, Bethesda, MD 20892, USA

²Laboratoire de Microbiologie et Génétique Moléculaires Centre, National de la Recherche Scientifique, 118 Route de Narbonne, 31062, Toulouse Cedex, France

³Present address: Department of Chemistry, University of Toledo, Toledo, OH 43606, USA.

⁴These authors contributed equally to this work.

*Correspondence: fred.dyda@nih.gov

DOI 10.1016/j.cell.2007.12.029

SUMMARY

The smallest known DNA transposases are those from the IS200/IS605 family. Here we show how the interplay of protein and DNA activates TnpA, the *Helicobacter pylori* IS608 transposase, for catalysis. First, transposon end binding causes a conformational change that aligns catalytically important protein residues within the active site. Subsequent precise cleavage at the left and right ends, the steps that liberate the transposon from its donor site, does not involve a site-specific DNA-binding domain. Rather, cleavage site recognition occurs by complementary base pairing with a TnpA-bound subterminal transposon DNA segment. Thus, the enzyme active site is constructed from elements of both protein and DNA, reminiscent of the interdependence of protein and RNA in the ribosome. Our structural results explain why the transposon ends are asymmetric and how the transposon selects a target site for integration, and they allow us to propose a molecular model for the entire transposition reaction.

INTRODUCTION

DNA transposition is a ubiquitous phenomenon occurring in all kingdoms of life during which discrete segments of DNA called transposons move from one genomic location to another. In both eukaryotes and prokaryotes, DNA transposition has been a significant part of evolution. Many eukaryotic genomes are littered with transposons or their inactive remnants (Lander et al., 2001), primarily scattered between genes. In bacteria, transposable elements can carry antibiotic resistance genes and, when combined with conjugation, are major drivers of broad genome remodeling and the emergence of antibiotic resistant strains. The discovery and engineering of DNA transposons active in vertebrate cells (Miskey et al., 2005) have led to their use in identifying

oncogenes and tumor suppressors and characterizing genes of unknown function, through their ability to disrupt genes or regulatory regions. They also have exciting potential as gene delivery systems for gene therapy applications.

A variety of structurally and mechanistically distinct transposase enzymes have evolved to carry out transposition by several different pathways (Curcio & Derbyshire, 2003). In all cases, these enzymes possess a nuclease activity that allows them to cleave DNA in order to excise transposon DNA which is subsequently spliced it into a new location. Depending on the system (Dyda et al., 1994; Grindley et al., 2006), different types of nucleophiles can be used by transposases to cleave DNA by attacking a phosphorus atom of a backbone phosphate group: water, generally activated by enzyme-bound metal ions; a hydroxyl group at the 5' or 3' end of a DNA strand; or a hydroxyl-group bearing amino acid in the active site of the transposase itself, such as serine or tyrosine. When a catalytic serine or tyrosine is used, the enzyme becomes attached to DNA through a covalent phosphoserine or phosphotyrosine bond.

One group of transposases that use catalytic tyrosines consists of the Y1 transposases (Ronning et al., 2005). These are members of a vast superfamily of nucleases characterized by a conserved His-hydrophobic-His (HUH) motif (Koonin & Ilyina, 1993) that provides two ligands to a divalent metal ion cofactor. HUH nucleases always cut a DNA strand with a polarity resulting in a 5' phosphotyrosine linkage and a free 3' OH group. In contrast to many HUH superfamily members, which are monomeric and have two catalytic tyrosines, Y1 transposases have only one catalytic tyrosine and form obligatory dimers (Ronning et al., 2005; Lee et al., 2006).

We have recently determined the structure of a Y1 transposase from the insertion sequence IS608 (Ronning et al., 2005), originally identified in *Helicobacter pylori* (Kersulyte et al., 2002), a bacterium that causes gastric inflammation leading to ulcers and occasionally to stomach cancer. ISs are the simplest autonomous transposable elements. While they tend to be short (<2.5 kb) and carry only those genes needed for transposition, if placed flanking a DNA segment, many are able to mobilize the intervening genes (Mahillon and Chandler, 1998). In addition to

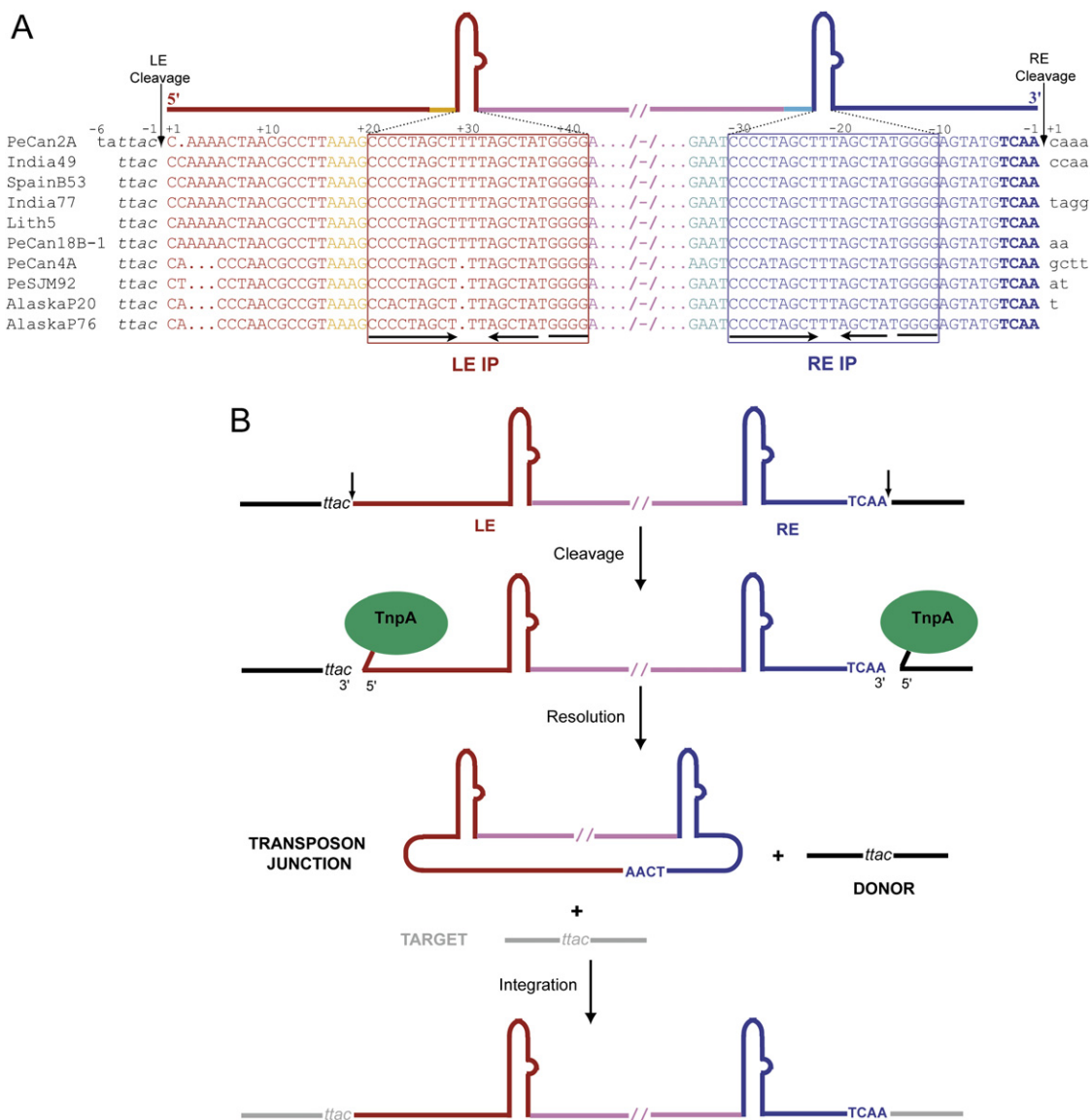


Figure 1. IS608 Transposition

(A) Alignment (adapted from Kersulyte et al. [2002]) of the termini and flanking sequences of IS608 elements from *Helicobacter pylori*. The strain is indicated on the left; all the work reported here was done with IS608 from PeCan2A (top line). Flanking DNA is in black, bases of the left end (LE) are shown in red and orange, and bases of the right end (RE) are shown in shades of blue. Boxed sequences underlined with inverted arrows delineate the imperfect palindromes (IP) at each end. The bases are numbered such that, at each end, the cleavage site is between base -1 and base+1 where bases 5' of the cleavage site are negative and those 3' are positive.

(B) Model of single-stranded transposition from Guynet et al. (2008). Intermediates in the reaction are a circular transposon junction and a precisely sealed donor backbone.

dispersing antibiotic resistance genes, IS transposition can indirectly lead to antibiotic-resistant bacterial strains. For example, a metronidazole-resistant strain of *H. pylori* has arisen because the nitroreductase gene needed for prodrug activation has been disrupted by an IS605-related transposition event (Debets-Ossenkopp et al., 1999).

ISs can be classified into groups or families based on the general features of their DNA sequences and associated transposases (<http://www-is.biotoul.fr>). A particularly interesting family

consists of the IS200/IS605 elements (Kersulyte et al., 2002), which do not have inverted sequences at their ends characteristic of many prokaryotic and eukaryotic transposons. Rather, imperfect palindromic (IP) sequences are located close to the transposon ends (Figure 1A). In the case of one family member IS608, the left end (LE) and right end (RE) have almost identical IP sequences that form DNA stem loop structures (Ronning et al., 2005). Intriguingly, these IPs are asymmetrically located: the IP at RE (IP_{RE}) is closer to the RE cleavage site at the transposon end than the IP at

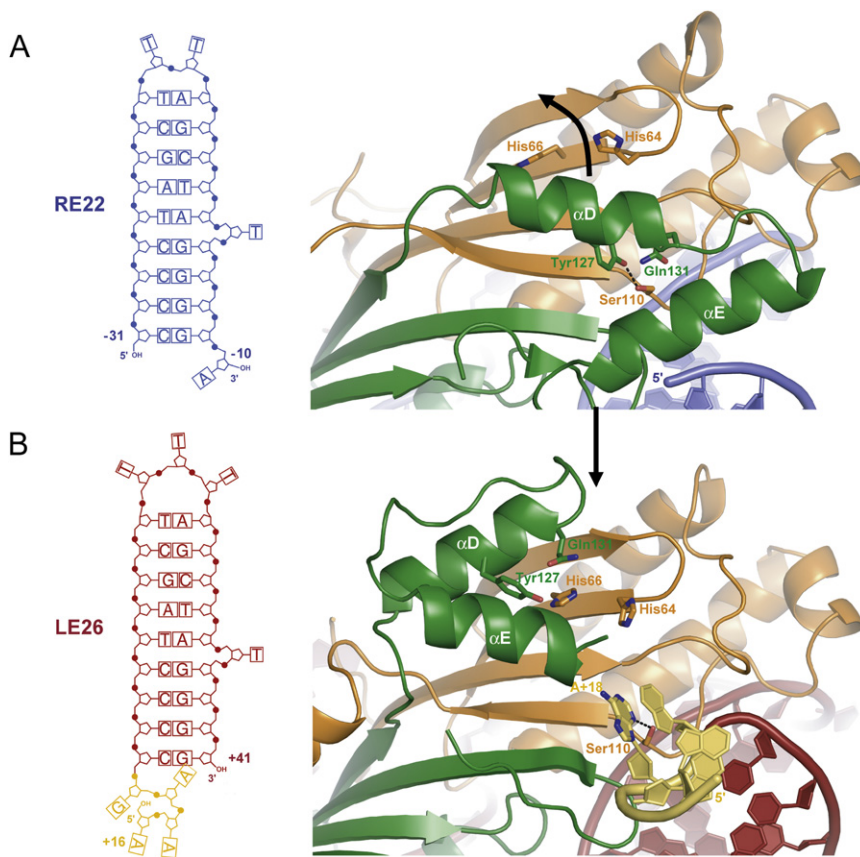


Figure 2. Conformational Change Induced in TnpA by a Four Nucleotide Extension of the IP

(A) Active site of TnpA bound to the RE22 hairpin (shown in blue). The two monomers of the TnpA dimer are colored green and orange. In this inactive conformation, the nucleophilic Y127 of one monomer is hydrogen bonded to Ser110 of the other. (B) The same region of TnpA when bound to LE26 (shown in red and yellow) in which the IP is extended by 4 nt in the 5' direction. Base A+18 has displaced Y127. Note that in the hairpin regions, LE and RE differ only by one T at the tip. The conformational change also necessarily shifts the residues that follow helix α D; we are only able to trace these in one of the monomers in the TnpA/LE26 structure.

LE (IP_{LE}) is to the LE cleavage site, and the nucleotide sequences between the IPs and the cleavage sites at the two ends are unrelated (Figure 1A). Among IS608 copies from different *H. pylori* strains, the sequence between IP_{RE} and the RE cleavage site is completely conserved, whereas it is variable between IP_{LE} and the LE cleavage site.

Another curious feature of IS200/IS605 family members is that, unlike many DNA transposons, which integrate essentially randomly, they always insert just 3' of a specific four or five nucleotide (nt) sequence. The form of IS608 that is inserted is an excised circular intermediate (also known as a transposon junction) (Figure 1B) in which the RE is linked directly to the LE (Guynet et al., 2008). Upon excision, IS608 precisely reseals the gap left behind in the donor DNA, and insertion occurs without target site duplications (Ton-Hoang et al., 2005). Thus, these seamless reactions proceed without loss or gain of nucleotides or the need for host cell DNA repair factors.

All IS608 cleavage and rejoining steps are carried out by a single 155 amino acid transposase, TnpA (Guynet et al., 2008). In the TnpA dimer, there are two active sites, assembled in *trans*, in which the tyrosine nucleophile of one monomer is near the HUH motif of the other. TnpA recognizes and cleaves only the top strand of each transposon end (Ton-Hoang et al., 2005), resulting in yet another level of asymmetry: due to the conserved polarity of cleavage, after nucleophilic attack by the active site tyrosine on the phosphodiester backbone of DNA at LE, TnpA is covalently linked to the transposon 5' end, whereas cleavage

at RE results in the attachment of TnpA to flanking donor DNA (Figure 1B).

We have previously shown how TnpA recognizes and pairs its transposon ends (Ronning et al., 2005), a necessary prelude to the cycle of coordinated DNA strand cleavage and rejoining steps that constitute transposition. Here, based on five different crystal structures of complexes between TnpA and various IS608 LE and RE sequences, and associated biochemical experiments, we describe the entire transposition cycle—activation

of TnpA upon end binding, recognition of the cleavage sites at the very edges of the transposon, and target site selection—and the absolute dependence of these steps on the inherent asymmetry of the transposon ends.

RESULTS

TnpA Complexes with the LE26 DNA Hairpin

We have previously described the crystal structures of TnpA alone and complexed with a 22-mer hairpin (RE22) representing IP_{RE} (Figure 2A; Ronning et al., 2005). While these were informative, in both structures, the catalytic tyrosine, Y127, was tucked away from the HUH motif and hydrogen-bonded to S110, where it could not act as a nucleophile. As there are several crystal structures of HUH nucleases with fully assembled active sites (Guasch et al., 2003; Larkin et al., 2005), it was clear that a conformational change was required. The other puzzling aspect of active site assembly was how the catalytically required metal ion would bind. In other HUH nuclease crystal structures, the metal cofactor (Mg²⁺ or Mn²⁺) is coordinated by three protein ligands: the two HUH histidines and either a third histidine or a glutamate, depending on the nuclease. Neither of our structures suggested an obvious candidate for the third metal ion ligand.

To shed light on these issues, we crystallized TnpA with a series of longer DNA substrates that contained the IPs and extended toward the transposon ends. (In our base-numbering convention [Figure 1], the cleavage site at each transposon end is between

base -1 and base $+1$. Base numbers increase with distance from the cleavage site with negative numbers on the 5' side of each cleavage site. Nucleotides [nt] flanking LE are italicized, and the last four nt on RE are in bold.) We first cocrystallized and solved the 2.1 Å resolution structure of TnpA complexed with a 26-mer hairpin DNA (LE26) representing IP_{LE} with a 4 nt 5' extension (Table S1 and Figure 2B). In the TnpA/LE26 complex, IP_{LE} binds precisely as seen for IP_{RE}. The only difference between IP_{LE} and IP_{RE}, an extra T in the LE hairpin loop, is turned toward the solvent and does not contact TnpA. However, as a consequence of adding 4 nt in the direction of the transposon end, there has been a major conformational change affecting both TnpA monomers in which helix α D carrying Y127 has swung across the face of the β sheet to adopt a completely new location (Movie S1 and Figure 2). The pivot point for the movement is around two residues, G117 and G118, in the loop immediately preceding helix α D (Figure S1). As a result of the helix movement, the nucleophilic -OH group of Y127 shifts 12 Å to a position now consistent with active site arrangements of other HUH nucleases.

The element of LE26 that appears to drive the conformational change in helix α D is base A+18 in the 4 nt 5' extension. In the TnpA/LE26 complex, the previously observed hydrogen bond between Y127 and S110 has been disrupted, and the space that had been occupied by Y127 in the TnpA/RE22 structure is now occupied by A+18 (Figure 2). The new hydrogen bond between A+18 and S110 is the only additional base-specific interaction that TnpA makes with LE26 when compared with RE22. The ability of A+18 to evict helix α D from its previous location is due in part to the dearth of interactions between helix α D and the rest of TnpA. In the TnpA/RE22 complex, helix α D is held in place by only one hydrogen bond and some scattered van der Waals contacts between hydrophobic groups. As a result of the intrusion of base A+18 in the TnpA/LE26 complex, the hydroxyl group of Y127 is no longer hydrogen bonded to anything and thus is ready to attack the scissile phosphate.

Another residue of interest located on helix α D is Q131, which is highly conserved among IS200 transposases and whose mutation to alanine dramatically reduces transposition in vivo (Figure S2). As a consequence of the conformational change in helix α D, Q131 is now close to the HUH histidines, where it appears appropriately placed to complete the divalent metal ion binding site. To test this, we soaked preformed TnpA/LE26 crystals overnight in buffer containing 5 mM MnCl₂ (Table S1). The anomalous difference Fourier electron density calculated from data measured on these crystals in the neighborhood of the active site indeed shows Mn²⁺ coordinated by H64, H66, and Q131 (Figure S2).

We also compared the metal ion binding affinity of TnpA/RE22 and TnpA/LE26 complexes using isothermal titration calorimetry. The experiments were performed with Mn²⁺, as our previous experience with an HUH nuclease suggested that Mn²⁺ might bind with higher affinity than Mg²⁺ (Hickman et al., 2002). As shown in Figure S2, TnpA/RE22 has no detectable affinity for Mn²⁺, whereas the divalent metal ion is clearly bound by TnpA/LE26. Consistent with the role of Q131 as the crucial third metal ion ligand, we cannot detect Mn²⁺ binding by the TnpA(Q131A)/LE26 complex. Taken together, these data indicate that the 4 nt 5' extension of LE26 relative to RE22 causes a rearrangement in TnpA leading to active site assembly in which Y127 and the third

metal ion ligand are simultaneously transported to where they are needed for catalysis.

Cleavage Activity of TnpA Is Dependent on the 4 nt 5' Extension of the IPs

Our observation that a short 5' extension of IP_{LE} causes a conformational change in TnpA that appears to assemble the active site led us to ask if, in the LE26-bound form, TnpA was competent for catalysis. We have previously shown that TnpA cleaves 70- and 80-mer ssDNA RE and LE substrates, which span the IPs and the cleavage sites (Ronning et al., 2005; Ton-Hoang et al., 2005). To investigate the effect of adding the 4 nt to IP sequences, we modified the cleavage reaction by providing the IPs and the cleavage sites on separate oligonucleotides. TnpA was first bound to oligonucleotides containing the IP sequences, with or without the 4 nt 5' extensions, and substrates that spanned the cleavage sites from bases -4 to $+4$ were then added. Upon cleavage, TnpA forms a phosphotyrosine link to the 4 nt on the 5' phosphate at the break (Ronning et al., 2005; Ton-Hoang et al., 2005), and the resulting covalent complexes can be detected by SDS-PAGE on the basis of the increase in the molecular weight of TnpA.

As shown in Figure 5A, on both LE (lanes 5 and 6) and RE (lanes 3 and 4), formation of covalent complexes between TnpA and the cleavage substrates is dependent on the 4 nt 5' extension. This is consistent with the crucial role of the additional nucleotides in inducing active site assembly. Furthermore, cleavage is dependent on the "correct" combination of LE and RE oligonucleotides: when IP_{LE} with the 4 nt 5' extension was mixed with the RE cleavage substrate (lane 9), or IP_{RE} with the 4 nt 5' extension was mixed with the LE cleavage substrate (lane 11), covalent complexes were not detected. This indicates that TnpA is able to differentiate between the LE and RE cleavage sites in a manner that depends on the particular IP bound.

RE31 and RE35 Complexes

To address how the transposon ends reach the TnpA active sites, we determined the 2.9 Å resolution structure of TnpA cocrystallized with a RE 31-mer (RE31) that contains IP_{RE} and the 10 nt in the 3' direction reaching the end of the transposon (Table S1). In marked contrast to the effect seen on LE where extending the IP sequence toward the LE cleavage site leads to TnpA activation, in the TnpA/RE31 complex, each TnpA monomer is in the inactive conformation. Although IP_{RE} is bound as seen in the TnpA/RE22 complex, the nucleotides 3' of IP_{RE} protrude out into solvent and become completely disordered after a few residues (Figure S3).

We therefore extended RE31 by adding 4 nt in the 5' direction. Cocrystals of TnpA bound to RE35 diffracted to 2.4 Å resolution (Table S1), and the structure revealed two important differences when compared to that of TnpA/RE31 (Figures 3A, 3B, and S3). First, the active site has been assembled: helix α D has undergone the conformational change seen in the TnpA/LE26 complex and Mn²⁺ that was included in the crystallization buffer is bound. Second, all RE35 nucleotides are ordered and the conformation is such that its 3' end, the last nt of RE, is now located in the active site.

In the TnpA/RE35 complex, RE35 resembles a distorted letter "C" in which IP_{RE} is bound on one side of TnpA, and the 4 nt 5'

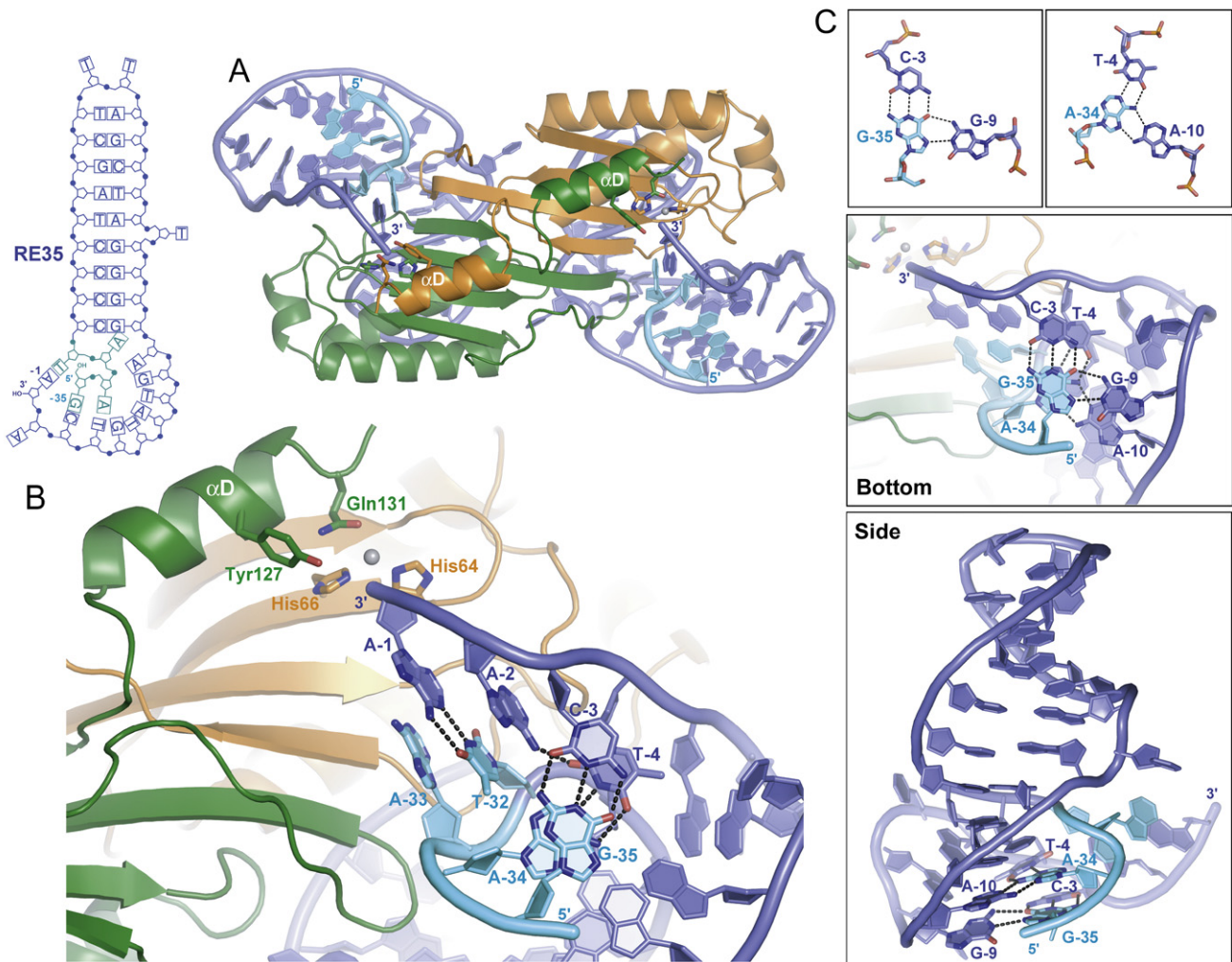


Figure 3. The IS608 Right End Is Directed into the TnpA Active Site by Internal DNA Interactions, Not by Protein-DNA Recognition

(A) Overall view of the TnpA/RE35 structure.

(B) Close-up of the active site showing the base pairs between the four bases at the RE of IS608 (**TCAA**) and bases 5' of IP_{RE} (GAAT) from base G-35 to T-32, in light blue. The gray sphere is bound Mn²⁺.

(C) Two base triplets (top) are central to the RE35 conformation (shown in two orthogonal views in the middle and bottom panels).

extension and the 10 nt that lead to the cleavage site both curl around the protein surface into the active site of the same monomer on the opposite face (Figure 3C). Furthermore, there are specific base-pairing interactions between the 4 nt 5' extension of the IP_{RE} and 3 nt at the 3' end of the transposon that direct the terminal 3' OH group, whose oxygen would be part of the scissile phosphate, into the active site (Figure 3B). The resulting arrangement of active site elements resembles the cocrystal structure of Tral, an HUH protein, bound to ssDNA that spans the F plasmid *nic* site in which the scissile phosphate was captured in the active site (Larkin et al., 2005).

A second important role of the 4 nt 5' extension of IP_{RE} is now clear: the last 4 nt of the transposon RE, **TCAA**, that immediately precede the cleavage site are held in place by a set of Watson-Crick base pairs with the 5' extension of IP_{RE} (Figure 3C). The base pairs (**A-1:T-32**, **C-3:G-35**, and **T-4:A-34**) do not match

up linearly in the transposon sequence, and the resulting twisted structure was unexpected. One base of the 5' extension, A-33, recapitulates the role of A+18 in the TnpA/LE26 complex in that it has displaced Y127 during the transition from the inactive to the active conformation and is now tucked into the pocket previously occupied by Y127.

Another surprising aspect of the way in which the 3' end of the transposon is brought into the active site is that two base pairs, **C-3:G-35** and **T-4:A-34**, are, in fact, part of base triplets (Figures 3C and S4). G-9, G-35, and **C-3** form a G-G-C triplet, which is stacked on the A-A-T triplet formed by A-10, A-34, and **T-4**. Although base triples have been frequently observed in RNA structures, to our knowledge, this is the first time DNA base triples have been observed bound to a protein in a biologically relevant context. An interesting question is whether RE folds by itself to achieve the observed configuration or it is induced by TnpA.

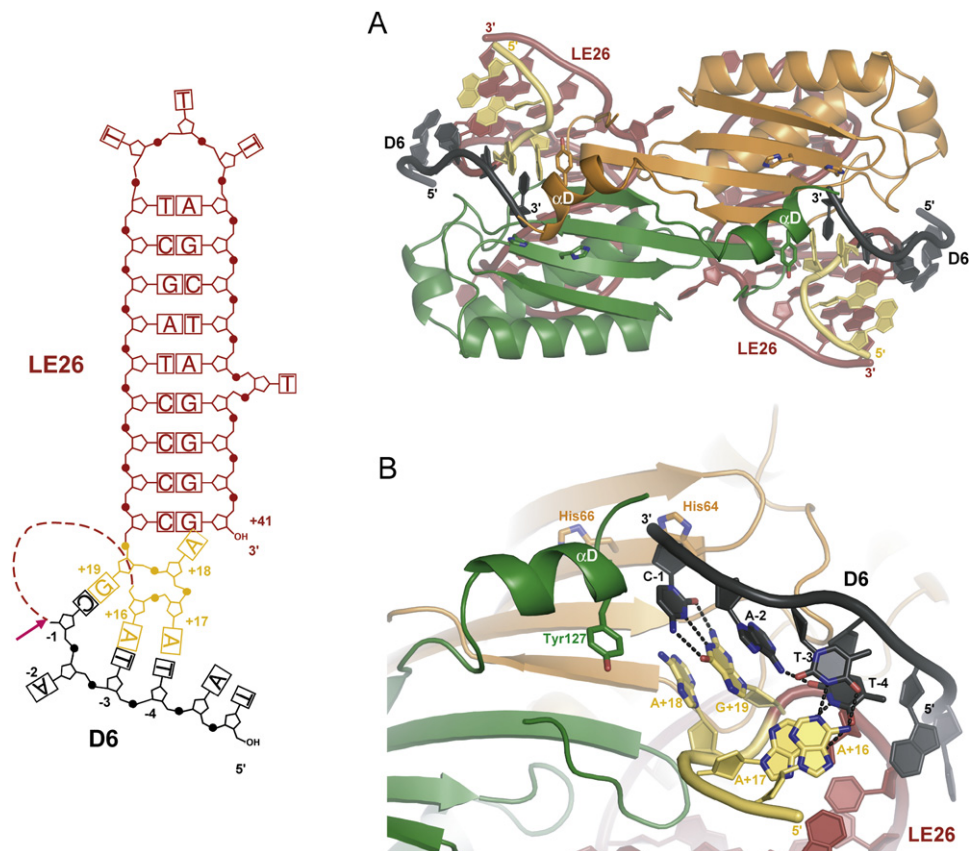


Figure 4. Ternary Complex of TnpA Bound to LE26 and the LE Donor Flank Echoes RE Recognition

(A) Overall view of the TnpA/LE26/D6 structure. On the left is a schematic of the oligonucleotides used where the dotted line indicates the break between LE26 and the donor flank, D6 (in black). The red arrow indicates the LE cleavage site.

(B) Close-up of the active site showing that, although the mode of interaction resembles the TnpA/RE35 structure, the specific bases differ.

The LE Ternary Complex

Attempts to cocrystallize TnpA with longer LE sequences that extend 5' from IP_{LE} to the LE cleavage site have thus far been unsuccessful, due to the poor biophysical properties of these complexes. However, the observation that IS608 always integrates precisely 3' of *TTAC* led us to explore the possibility that this sequence might somehow be recognized by TnpA. Although short *TTAC*-containing oligonucleotides do not bind to TnpA on their own, they do so in the presence of LE26 (data not shown), and we obtained crystals of TnpA bound to LE26 and the 6-mer *TATTAC* (denoted D6) that diffracted to 1.9 Å resolution (Table S1).

In the ternary LE complex, we observe the *TTAC* bases of D6 in the same position and orientation as the *TCAA* bases at the very end of RE35 in the TnpA/RE35 complex. The *TTAC* tetranucleotide is located in the active site, where it is held in place by the 4 nt 5' extension of IP_{LE} (Figure 4). In this case, base pairs occur between A+16:T-3, A+17:T-4, and G+19:C-1 (Figure 4B). These orient the scissile phosphate (whose position can be inferred from the terminal 3' OH group of D6) for nucleophilic attack by Y127. The overall DNA conformation is very similar to that seen in TnpA/RE35, except that the nucleotides between the cleavage site and LE26 are missing; the analogous regions of the

TnpA/LE26/D6 and TnpA/RE35 complexes are virtually superimposable.

The observation that the LE ternary complex structurally echoes the TnpA/RE35 complex is explained by the conserved polarity of the cleavage reactions. Although the interactions are similar on both ends, the flanking *TTAC* sequence recognized by the 4 nt 5' extension of IP_{LE} differs from the transposon 3' end *TCAA* sequence that is recognized by the IP_{RE} 5' extension. The key is that the compensating changes to retain Watson-Crick base pairing are present in the 5' extensions of the IPs.

In the TnpA/LE26/D6 complex, helix α D appears in yet another inactive position away from the active site. We suspect this is a crystallization artifact, as the activated position of helix α D is blocked by a crystal lattice contact, and we know that, in solution, helix α D is able to adopt the activated conformation in LE ternary complexes as TnpA prebound to LE26 can cleave an 8-mer that spans the cleavage site (Figure 5A). The previously seen inactive conformation (Ronning et al., 2005) is also unavailable as base A+18 of LE26 occupies the pocket where Y127 sits in uncomplexed TnpA and in the TnpA/RE22 and TnpA/RE31 complexes. Finally, the relevance of the observed position of helix α D in the TnpA/LE26/D6 complex is suspect as any extension of D6 in the 3' direction (i.e., uncleaved LE) would immediately be

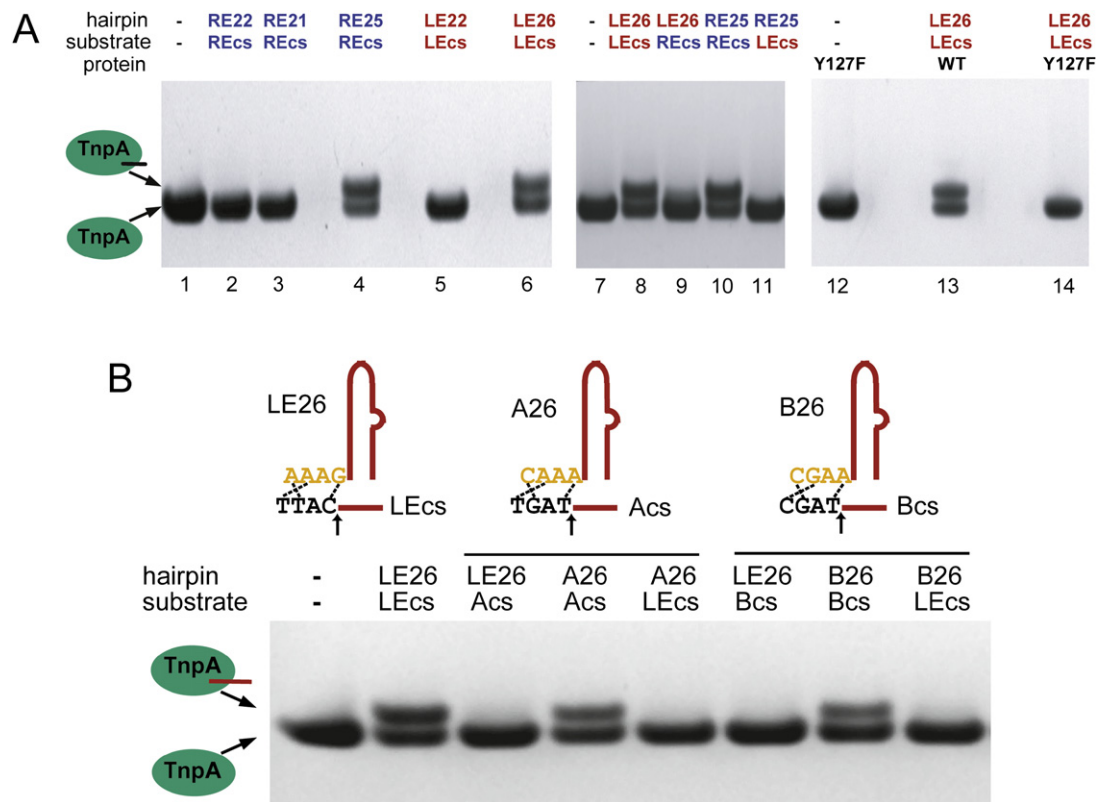


Figure 5. Transposon End Cleavage Can Be Redirected

(A) SDS-PAGE gel showing the results of cleavage assays. Upon cleavage of an 8-mer that spans the LE and RE cleavage sites, TnpA (green oval) becomes covalently attached to 4 nt and can be resolved from unmodified TnpA. TnpA cleaves LE and RE cleavage substrates (cs) only when the appropriate 5' extension is added to IP sequences. No covalent complex is formed with the Y127F active site mutant.

(B) Modification of cleavage specificity. Shown are the results of LE cleavage assays using LE26 and LEcs and two variants.

in steric conflict with helix α D. This variability in the position of helix α D adds to the body of data that suggests it is a mobile structural element that tends to wander (Figure S5).

We note that the TnpA/LE26/D6 structure represents not only how TnpA recognizes its LE cleavage site but also how a TTAC-containing target site is captured. Since the circular transposon intermediate that can be integrated into target DNA, a transposon junction (Guynet et al., 2008), contains the LE26 sequence but not the LE TTAC flank (Figure 1B), TnpA bound to the transposon junction is capable of binding (and subsequently cleaving) a TTAC-containing target. Therefore, recognition of TTAC of the target and of the LE flank is identical.

Changing Cleavage Specificity

The recognition of the integration target DNA sequence by protein-bound transposon DNA, rather than by TnpA directly, raises the obvious possibility that TnpA-catalyzed insertions might readily be retargeted to other tetranucleotide sequences. This seems possible in principle, as three of the four nucleotides in the 5' extensions of the IPs do not appear to play any role beyond recognizing TTAC on LE or TCAA on RE. Thus, their replacement should not impede transposition.

To test the potential for redirecting, we changed either two or three of the nucleotides in the 5' extension of IP_{LE} and introduced

the compensating base-pairing partners in 8-mer cleavage substrates (which represent both the LE cleavage site and the target site). In the variant 5' extensions, A+18 was retained, as its role is to displace Y127 from its inactive location, and it is not involved in DNA recognition. As shown in Figure 5B for two variant target sites, the cleavage specificity of TnpA can indeed be effectively changed, and we are in the process of examining transposon re-targeting in vivo.

Substrate Cleavage and Junction Formation by Active Site Mutants of TnpA

All our crystal structures of TnpA show the dimer in a *trans*-active site configuration in which Y127 of one monomer is close to the HUH motif of the other. To confirm that this shared active site arrangement is used during catalysis, we performed several types of in vitro assays, which recapitulate biochemical steps of IS608 transposition (Guynet et al., 2008) using mixtures of single active site mutant versions of TnpA. We reasoned that if the shared active site arrangement is indeed used, mixing an inactive Y127F mutant with an inactive H64A mutant should result in measurable activity, as any heterodimers would have one active site that combines the H64A and Y127F mutations yet the other would have the HUH motif and Y127 intact (Figure 6A).

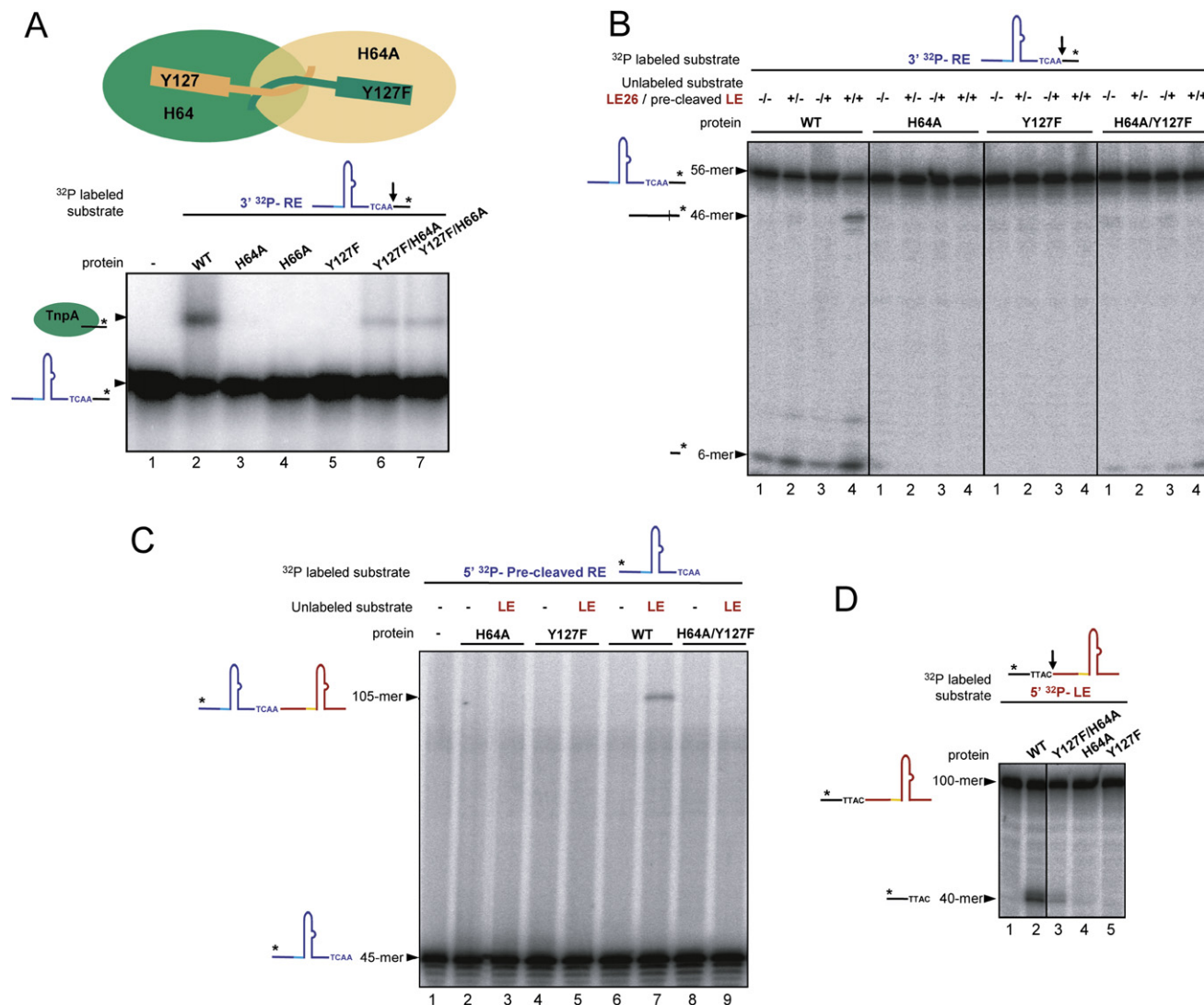


Figure 6. Mixed Mutant Dimers Suggest Transposon End Cleavage Is In *trans* and Resolution Is In *cis*

(A) Results of RE cleavage assays using mixed active site point mutants. The radiolabeled oligonucleotide is detected.

(B) RE cleavage and donor backbone formation by mixed active site mutants was assessed by mixing a RE cleavage substrate (56-mer) with a LE flank (40-mer). The product of RE cleavage is a 6-mer, and the 46-mer is the sealed donor backbone that forms between the LE flank and the RE cleavage product.

(C) Transposon junction formation by mixed active site mutants was assessed by mixing a LE cleavage substrate (100-mer, which is cleaved to yield a 60-mer transposon LE) with a precleaved transposon RE (45-mer). The transposon junction is formed by the WT protein (lane 7) but not by mixed active site mutants (lane 9).

(D) LE cleavage is catalyzed by mixed active site mutants (lane 3), but not by the single point mutants (lanes 4 and 5).

Figure 6A shows the results of RE cleavage experiments in which a 56-mer RE substrate that includes six flanking nucleotides is incubated with wild-type TnpA, single active site point mutants, or mixed active site mutants. As expected (Ronning et al., 2005), no covalent products are observed with the H64A, H66A, or Y127F mutants (lanes 3–5). However, when the Y127A and H64A or H66A mutants are mixed, a covalent complex between TnpA and the 6-mer cleavage product can be detected (lanes 6 and 7), suggesting that a catalytically competent *trans*-active site has assembled. The 6-mer product can also be directly detected after digestion with proteinase K. As shown in Figure 6B,

in control experiments with the 56-mer RE cleavage substrate, wild-type TnpA generates the 6-mer product, whereas the Y127F and H64A mutants do not (lane 1 in first three panels). However, mixing these mutants results in the cleavage of the RE substrate to generate the 6-mer (fourth panel, lane 1), consistent with a *trans*-active site configuration.

One of the hallmarks of IS608 transposition is that, upon transposon excision, the donor backbone is precisely sealed (Figure 1B). To determine whether mixed mutant dimers can generate sealed donor backbones, the 56-mer RE cleavage substrate with six flanking nucleotides was mixed with a 40-mer LE

backbone (i.e., 40 nt of flanking sequence ending with *TTAC*-3') in the presence of LE26. The LE donor substrate is necessarily precleaved since, in the mixed mutant dimers, only one active site is functional; LE26 is also required because the 5' extension of its IP is needed to localize the *TTAC* of the LE donor substrate in the active site. As shown in Figure 6B, wild-type TnpA covalently joins the 40-mer LE donor substrate to the 6-mer product of RE cleavage to produce a 46-mer sealed donor backbone (panel 1, lane 4), but no such product is observed with the mixed mutant dimers (panel 4, lane 4).

Another reaction that occurs during IS608 transposition is the formation of a circular intermediate (Figure 1B) in which RE is linked directly to LE (Ton-Hoang et al., 2005). To test whether mixed mutant dimers can form such transposon junctions, we mixed a precleaved 45-mer RE substrate that ends in **TCAA**-3', representing the product of RE cleavage on the transposon side, with a 100-mer LE cleavage substrate that contains 60 nt of LE flanked by 40 nt (Figure 6C). Wild-type TnpA (lane 7) produces 105-mer junctions by catalyzing the attack of the RE 3' OH of **TCAA** on the LE 5' phosphotyrosine linkage that is formed upon LE cleavage. While mixed mutant dimers can cleave LE (Figure 6D, lane 3), junctions cannot be detected (Figure 6C, lane 9).

These observations show that, while mixed mutant dimers can cleave both LE and RE, a result consistent with a *trans*-active site arrangement for cleavage, they cannot form sealed donor backbones or transposon junctions. This suggests that the mixed mutant dimers are deficient in the resolution steps of transposition, as they are unable to resolve phosphotyrosine intermediates to form the appropriately joined products.

DISCUSSION

The overwhelming body of evidence indicates that IS608 transposes using ssDNA (Kersulyte et al., 2002; Ton-Hoang et al., 2005; Ronning et al., 2005), and we have recently shown that ssDNA LE and RE oligonucleotides are readily cleaved, form transposon junctions and sealed donor backbones, and integrate preformed transposon junctions into target DNA in the presence of TnpA (Guynet et al., 2008). With our structural results demonstrating how TnpA is activated and how it recognizes the transposon ends and its cleavage sites, together with the observation that helix α D is a mobile structural unit, we propose the following model for IS608 transposition (Figure 7 and Movie S2):

Transposition starts with TnpA locating and pairing the transposon ends by binding to the hairpins formed by the top strand LE and RE IPs (Figure 7A). IP_{LE} and IP_{RE} differ by only one base in the hairpin loop, and our structures of the TnpA dimer bound to two identical DNA molecules most likely reliably reflect features of TnpA bound to one IP_{LE} and one IP_{RE}. Binding the transposon IPs induces the conformational change seen in the TnpA/LE26 complex, during which helix α D moves into the activated position thereby assembling the active site.

Divalent metal ion binding to the assembled active site localizes and polarizes the scissile phosphate, preparing it for nucleophilic attack by Y127 (Hickman et al., 2002; Larkin et al., 2005). On LE, upon cleavage (Figure 7B), Y127 becomes covalently linked to the 5' end of the transposon, while the 3' end of flanking

donor remains bound through base-base interactions between its *TTAC* and the 4 nt just 5' of IP_{LE} (as in the TnpA/LE26/D6 complex). We have no evidence that the 15 transposon nt between this 5' extension and the 5' end of the transposon interact with TnpA, consistent with their variability among different IS608 isolates (Kersulyte et al., 2002).

On RE, cleavage results in a 5' phosphotyrosine linkage between Y127 and the flanking donor DNA, while the 3' end of the transposon stays bound through base-pairing interactions between the terminal **TCAA** tetranucleotide and the 4 nt 5' extension of IP_{RE} (as in the TnpA/RE35 complex) (Figure 7B). The entire RE (represented by RE35) is ordered, and its DNA conformation is stabilized by internal hydrogen bonds, consistent with its complete sequence conservation.

The subsequent formation of the transposition intermediates, a transposon junction and the sealed donor backbone, would arise straightforwardly if the two α D helices now trade places, pivoting on G117 and G118 and bringing the covalently linked DNA strands with them (Figure 7C and Movie S2). This model requires the 3' OH groups to remain in their "active sites of origin" to act as the nucleophiles to resolve the swapped phosphotyrosine linkages. This immobility seems likely as our structures of both LE and the RE complexes suggest that 3' ends would remain bound as long as the IPs with their 4 nt 5' extensions are present.

By this mechanism, in one active site of the dimer, a sealed donor backbone would be generated by nucleophilic attack by the stationary LE donor flanking 3' OH (*TTAC*-OH) on the swapped RE donor flank 5' phosphotyrosine linkage. In the other active site, attack by the resident RE 3' OH (**TCAA**-OH) on the 5' phosphotyrosine linkage of the swapped transposon LE would result in a transposon junction. This proposed reaction scheme is supported by the three previously unexplainable aspects of asymmetry seen at the transposon ends: (1) the tolerance of sequence variability at LE but not at RE; (2) the cleavage polarities that dictate that one phosphotyrosine linkage joins TnpA to the transposon end whereas the other covalently attaches TnpA to flanking DNA; and, finally, (3) the spacing differences between the cleavage sites and the IPs. On RE, upon cleavage TnpA becomes attached to the RE flank, which is part of the donor plasmid and presumably can move freely. It is therefore easy to imagine that the traveling helix α D can bring covalently attached flanking DNA to the adjacent active site. However, on LE, it is the transposon 5' end that is attached to helix α D. Thus, LE must have a sufficiently long and flexible spacer between the 4 nt IP_{LE} extension and the 5' end of the transposon that can act as a tether with some slack so helix α D can move from one active site to the other. The slack is necessary because LE cannot move as a unit, as it is anchored to the TnpA dimer by the IP_{LE} hairpin.

The notion of a switch from the *trans* to a *cis* active site arrangement is supported by the crystal structure (PDB ID 2fyx) of a closely related transposase from *Deinococcus radiodurans*, which was captured in the inactive configuration but with a *cis* helix α D arrangement. Although we have no structural evidence that the *cis* configuration occurs during IS608 transposition, our biochemical data showing that mixed mutant dimers are defective in the resolution steps provides strong support that both transposon junction and sealed backbone formation occurs with helix α D in *cis*: in this configuration, mixed mutant dimers

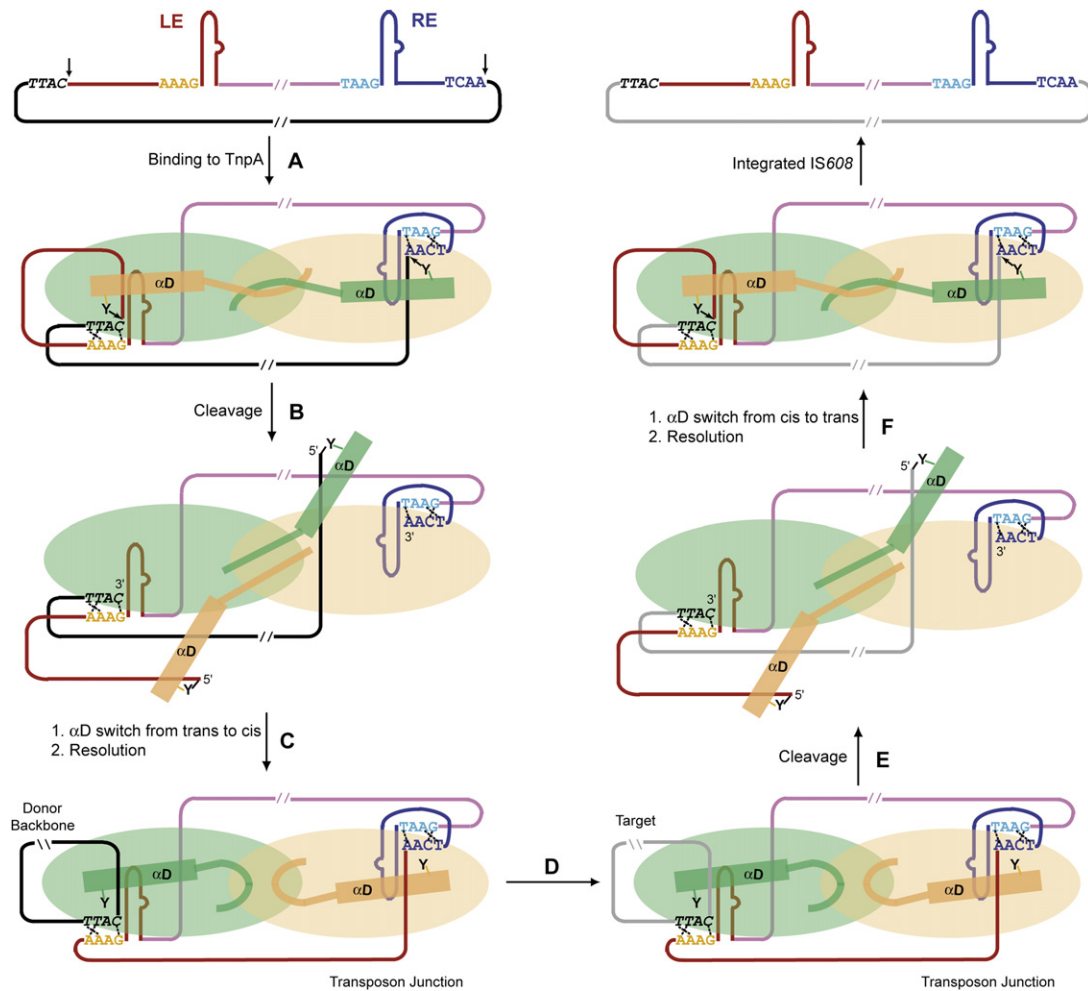


Figure 7. Model for IS608 Transposition

(A–F) Upon LE and RE binding (A), Y127 of each monomer cleaves the transposon ends and becomes covalently attached to the 5' side of the gap (B). Movement of α D helices from *trans* to *cis* and resolution of the phosphotyrosine intermediates results in a transposon junction and a sealed donor backbone (C). For integration (D), the donor backbone is replaced by target DNA containing TTAC which is recognized by an element of LE DNA. Cleavage (E), movement of the α D helices, and resolution of the phosphotyrosine intermediates (F) results in transposon insertion into target DNA immediately 3' of TTAC.

have no functional active sites. As shown in *Movie S2*, the switch of helices from one active site to the other can be easily modeled as long as the RE flank and the nucleotides between IP_{LE} and the LE cleavage site are free to move.

For the next step, integration, we do not know if the excised transposon junction intermediate remains bound to TnpA or is released and rebound. If, during recombination, the junction is released upon formation, it seems likely that TnpA resets to the *trans* configuration before transposon junction recapture, as we have only observed uncomplexed TnpA in that state. If the transposon junction stays bound, the cleavage steps required for integration may start with TnpA in the *cis* configuration and switch to *trans* for resolution. From the point of view of the overall mechanism, the outcomes of these two possibilities are equivalent.

We propose that integration of a transposon junction intermediate into a TTAC-containing target is a mechanistic replay of excision. After transposon junction formation, the sealed donor backbone dissociates from the complex and is replaced by

a TTAC-containing target sequence (Figure 7D). At one active site, the target DNA would bind through interactions between its TTAC tetranucleotide and the 4 nt 5' extension of IP_{LE} . Upon cleavage (Figure 7E), the TTAC target flank would stay bound to the complex, and the 5' end would be covalently attached to Y127. At the other active site, the transposon junction would be cleaved, leaving TCAA (the RE 3' end of IS608) bound to the active site and the LE (5' end of IS608) linked through a 5' phosphotyrosine linkage to Y127. A switch in the active site arrangements leads directly to the resolution steps in which the top strand of IS608 is inserted into a new target site: the stationary 3' OH of the TTAC target flank attacks the swapped 5' phosphotyrosine link at LE, while the RE TCAA 3' OH attacks the swapped 5' phosphotyrosine linkage of the target flank that was created during target cleavage (Figure 7F).

One of the most baffling questions about IS608 transposition was how its transposase, a 155-residue, single-domain protein, could carry out all of the required steps. Part of the answer is that

TnpA is sneakier than we thought: it uses bound transposon DNA to recognize its cleavage sites both on donor and target DNA obviating the need for an additional DNA binding domain. Furthermore, TnpA works only on one DNA strand and does not have to deal with the complementary strand (Kersulyte et al., 2002; Ton-Hoang et al., 2005; Ronning et al., 2005; Guynet et al., 2008).

If TnpA acts solely on ssDNA, how do its substrates arise? ssDNA formation might be promoted by plasmid supercoiling combined with the propensity of the IPs to form stem loops; if this occurs, the cleavage sites might, with some frequency, dissociate from their complementary strands. On the other hand, IS608 might excise in vivo only when DNA becomes single stranded during a normal cellular process such as lagging strand synthesis. If transposition occurs only during DNA replication, excised TnpA-bound sealed transposon circles might readily find a suitable TTAC-containing ssDNA target. Restricting transposition to one stage in the cell cycle would also ensure that the reaction is substrate-limited, thus preventing wanton and possibly destructive movement. Since ssDNA is also generated during conjugative DNA transfer, conjugating plasmids might be preferred targets for IS608 with the added advantage of immediate horizontal transfer.

The importance of ssDNA substrates for IS200 transposition is illustrated by recent work on *Deinococcus radiodurans*, which can survive severe ionizing radiation damage using a mechanism called “extended synthesis-dependent strand annealing” to reconstitute its shattered chromosomes (Zahradka et al., 2006). During recovery, as much as 15% of newly synthesized DNA is single stranded and, remarkably, the transposition frequency of ISDra2, an IS200/IS605 family member, increases 500-fold (Mennecier et al., 2006), suggesting that ssDNA is normally rate limiting.

One of our most surprising results is that IS608 uses DNA sequences in the transposon itself to recognize its cleavage sites. This mode of recognition suggests that TnpA may be redirected to new target sites, opening up an unanticipated avenue of transposon targeting with an array of genomic and biotechnological applications.

The interdependence of protein and DNA in creating suitable substrates is reminiscent of the intertwining of protein and RNA in ribosomes (Noller, 2005). This “self-recognition” has also been reported in other RNA-dependent systems. For example, the structural basis of the matchmaking functions of mitochondrial RNA-binding proteins (MRPs) has recently been reported (Schumacher et al., 2006).

There is a striking parallel between the IS608 transposition pathway and the mobility of group II introns, particularly with that of the bacterial L1.LtrB system (Belfort et al., 2002; Lambowitz and Zimmerly, 2004). For example, the mobility of RNA introns is dependent on an intron-encoded multifunctional protein, which is needed to bind the RNA. Upon splicing, exons bordering the intron are joined to each other, reminiscent of the resealing of donor DNA ends by TnpA. The lariat intermediate formed during intron splicing is similar to the circular IS608 transposon junction intermediate, both of which are covalently sealed. Perhaps the most significant parallel involves targeting, as these introns select their target, or “retrohoming” site, by base-pairing interactions between segments of the lariat intermediate and the target

DNA strand. This is the basis for the development of retargeted introns (Karberg et al., 2001) that can be used to disrupt chromosomal genes. In intron mobility, the key catalytic component is the RNA itself, which catalyzes both the splicing and reverse splicing events. Because DNA has no known self-cleavage and strand transfer activity, IS608 has to rely on the assistance of TnpA to carry out the necessary cleavage and joining reactions. Our work demonstrates that a targeting mechanism previously thought to be the property of RNA-based mobile systems also occurs in the context of a mobile DNA element.

From a structural and functional perspective, the closest characterized relatives of TnpA are IS91-related transposases (Garcillán-Barcia et al., 2001). These are widespread in bacteria, have eukaryotic homologs (Kapitonov and Jurka, 2001), and have been implicated in the movement of so-called Common Regions (Stokes et al., 1997; Toleman et al., 2006), which may be responsible for a large fraction of the spread of antibiotic resistance genes. While IS91-like elements transpose by a mechanism that is likely different from that of IS608, they also contain subterminal IPs and insert just 3' of short conserved sequences. It will be interesting to determine if their mode of target recognition resembles that shown here for IS608. If so, the potential for their retargeting could provide new possibilities toward the site-specific modification of eukaryotic genomes.

EXPERIMENTAL PROCEDURES

Protein Purification and Crystallization

TnpA was purified as previously described (Ronning et al., 2005). DNA was synthesized on an Applied Biosciences 394 DNA/RNA synthesizer or purchased from IDT (Coralville, IA). Sequences used for crystallization are shown in Figures 2–4. Oligonucleotides containing inverted repeat sequences were resuspended in TE, heated to 95°C for 15 min, and then rapidly cooled on ice and placed at –20°C until use. All crystals were obtained by vapor diffusion in hanging drops by mixing complexes 1:0.8–1.0 (v/v) with well solutions as described below. TnpA/LE26 crystals were frozen in paratone, and the rest were flash frozen in liquid propane.

TnpA/LE26: TnpA at 8 mg/ml was mixed with LE26 at a final protein:DNA molar ratio of 1:1.1 and dialyzed against 20 mM Tris pH 7.5, 0.3 M sodium malonate, 0.2 mM TCEP, and 2 mM EDTA. Well solutions consisted of 0.2 M sodium formate and 15%–20% PEG 3350.

TnpA/RE31: TnpA at 5 mg/ml was mixed with RE31 at a molar ratio of 1:1.1 and dialyzed against 20 mM Tris pH 7.5, 0.2 M sodium malonate, 10 mM MnCl₂, and 0.2 mM TCEP. Well solutions consisted of 15%–20% PEG 3350 and 0.1 M MES pH 6.5. Crystals were cryoprotected using well solution supplemented with 10% glycerol.

TnpA/RE35: The complex was prepared as for TnpA/RE31, and the well solution consisted of 20%–25% PEG 3350, 0.1 M MES pH 5.5, and 0.1 M ammonium acetate. Crystals were frozen after stepwise replacement of water for 10% glycerol in the mother liquor.

TnpA/LE26/D6: TnpA (5 mg/ml) was mixed with LE26 and D6 at a 1:1.1:1.3 molar ratio, dialyzed against 20 mM Tris pH 7.5, 0.2 M MgCl₂, 0.2 mM TCEP, and mixed with well solutions consisting of 6%–10% PEG 600 and 50 mM sodium citrate pH 5.0. Crystals were cryoprotected by transfer into 10% PEG 600, 0.1 M MgCl₂, 25 mM sodium citrate, 10 mM Tris pH 7.5, and 15% glycerol.

Data Collection and Structure Determination

Data on the TnpA/LE26 and TnpA/RE31 crystals were collected on beamline 22-ID at APS on a MAR300 CCD detector. All other diffraction data were collected at 95 K on a rotating anode source equipped with multilayer focusing optics using Cu K α radiation and a Raxis IV image plate detector. Data were integrated and scaled with Denzo and Scalepack (Otwinowski and Minor, 1997) (Table S1). The structures were solved with molecular replacement by

AMoRe (Navaza, 2001), providing clear solutions in all cases. Search models and solution statistics are in Table S1, as are refinement statistics. For refinement, manual model building with program O (Jones et al., 1991) was alternated with cartesian simulated annealing, positional and restrained B factor refinement cycles using CNS 1.1 (Brünger et al., 1998). TnpA residues 133–155 could not be traced in the RE31, RE35, and LE26/D6 complexes. In the LE26 and LE26/Mn²⁺ complex structures, all protein residues could be included in one monomer. Both LE26 complexes showed weak electron densities and high temperature factors for residues 132–141 between helices α D and α E, suggesting high mobility. All molecular figures and animations were made with PyMOL (DeLano, 2002).

Isothermal Titration Calorimetry (ITC)

Complexes of TnpA and TnpA/Q131A prebound to RE22 or LE26 (TnpA concentration of 0.035–0.038 mM) were prepared by dialysis against 10 mM HEPES pH 7.5, 0.2 M NaCl, 5 mM DTT, 5 mM MgCl₂, and 10% glycerol. Mn²⁺ binding was measured by ITC as described (Hickman et al., 2002), except that aliquots of 2 μ l MnCl₂ (5 mM in dialysis buffer) were used.

Covalent Complex Formation

Wild-type or the Y127F mutant TnpA at 1 mg/ml was mixed with hairpin oligos and cleavage substrates at a final protein:DNA molar ratio of 1:1.1:1.1. Protein/hairpin mixtures were dialyzed overnight against 20 mM, Tris pH 7.5, 0.2 M sodium malonate, 20 mM MgCl₂, prior to addition of the substrate, and incubation for 1 hr at 20°C. Samples were heat denatured in SDS-containing sample buffers and analyzed on 4%–12% SDS-PAGE gels. TnpA and TnpA attached to the 4-mer product of cleavage were detected by Coomassie staining (Figure 5).

Purification of Mixed TnpA Mutants and Activity Assays

Each point mutant (Y127F, H64A, H66A) was introduced into pBS107, expressed in *E. coli* Rosetta (DE3) cells (Novagen), and separately purified as previously described (Ton-Hoang et al., 2005). To form mixed mutant dimers, equimolar amounts of either Y127F and H64A or Y127F and H66A were incubated together on ice for 20 min. RE cleavage reactions (Figure 6A) were performed by 30 min incubation at 37°C of 28 nM of a 3'-³²P-labeled RE 56-mer cleavage substrate (see Supplemental Data for sequence) with 10 μ M of total protein in a final volume of 10 μ l in 20 mM HEPES at pH 7.5, 160 mM NaCl, 5 mM MgCl₂, 10 mM DTT, 20 μ g/ml BSA, 0.5 μ g of poly-dIdC, and 20% glycerol. Reaction products were separated on a 16% SDS-PAGE gel and subsequently analyzed by phosphorimaging. Similar reaction conditions (Guynet et al., 2008) were used for RE cleavage and donor backbone formation (Figure 6B), transposon junction formation (Figure 6C), and LE cleavage (Figure 6D). All DNA sequences are listed in Supplemental Data. Products were separated on an 8% sequencing gel and analyzed by phosphorimaging.

Supplemental Data

Supplemental Data include five figures, one table, and two movies and can be found with this article online at <http://www.cell.com/cgi/content/full/132/2/208/DC1/>.

ACKNOWLEDGMENTS

This work was supported in part by the Intramural Program of the National Institute of Diabetes, Digestive, and Kidney Diseases of the NIH. The Chandler lab was supported by CNRS (France) and EU contract LSHM-CT-2005-019023. C.G. received a training grant from the French MENRT. Data were also collected at the SER-CAT 22-ID beamline at the Advanced Photon Source, Argonne National Laboratory. Use of the APS was supported by the US Department of Energy, Basic Energy Sciences, Office of Science, under Contract No. W-31-109-Eng-38. We thank Dr. Wei Yang for insightful comments.

Received: August 19, 2007

Revised: October 28, 2007

Accepted: December 7, 2007

Published: January 24, 2008

REFERENCES

- Belfort, M., Derbyshire, V., Parker, M.M., Cousineau, B., and Lambowitz, A.M. (2002). Mobile introns: Pathways and proteins in mobile DNA II. D.N.A. Mobile, II, N.L. Craig, R. Craigie, M. Gellert, and A.M. Lambowitz, eds. (Washington, D.C.: ASM Press), pp. 761–783.
- Brünger, A.T., Adams, P.D., Clore, G.M., Delano, W.L., Gros, P., Grosse-Kunstleve, R.W., Jiang, J.S., Kuszewski, J., Nilges, M., Pannu, N.S., et al. (1998). Crystallography and Nmr System - a New Software Suite For Macromolecular Structure Determination. *Acta Crystallogr. D Biol. Crystallogr.* 54, 905–921.
- Curcio, M.J., and Derbyshire, K.M. (2003). The outs and ins of transposition: From Mu to kangaroo. *Nat. Rev. Mol. Cell Biol.* 4, 1–13.
- Debets-Ossenkopp, Y.J., Pot, R.G.J., van Westerloo, D.J., Goodwin, A., Vandebroucke-Grauls, C.M.J.E., Berg, D.E., Hoffman, P.S., and Kusters, J.G. (1999). Insertion of mini-IS605 and deletion of adjacent sequences in the nitroreductase (*rdxA*) gene cause metronidazole resistance in *Helicobacter pylori* NCTC11637. *Antimicrob. Agents Chemother.* 43, 2657–2662.
- DeLano, W.L. (2002). The PyMOL Molecular Graphics System at www.pymol.org.
- Dyda, F., Hickman, A.B., Jenkins, T.M., Engelman, A., Craigie, R., and Davies, D.R. (1994). Crystal structure of the catalytic domain of HIV-1 integrase: similarity to other polynucleotidyl transferases. *Science* 266, 1981–1986.
- Garcillán-Barcia, M., Bernales, I., Mendiola, M.V., and de la Cruz, F. (2001). Single-stranded DNA intermediates in IS91 rolling-circle transposition. *Mol. Microbiol.* 39, 494–501.
- Grindley, N.D.F., Whiteson, K.L., and Rice, P.A. (2006). Mechanisms of site-specific recombination. *Annu. Rev. Biochem.* 75, 567–605.
- Guasch, A., Lucas, M., Moncalian, G., Cabezas, M., Perez-Luque, R., Gomis-Ruth, F.X., de la Cruz, F., and Coll, M. (2003). Recognition and processing of the origin of transfer DNA by conjugative relaxase TrwC. *Nat. Struct. Biol.* 10, 1002–1010.
- Guynet, C., Hickman, A.B., Barabas, O., Dyda, F., Chandler, M., and Ton-Hoang, B. (2008). Single-stranded transposition of IS608: In vitro reconstitution of a new transposition mechanism. *Mol. Cell*, in press.
- Hickman, A.B., Ronning, D.R., Kotin, R.M., and Dyda, F. (2002). Structural unity among viral origin binding proteins: crystal structure of the nuclease domain of adeno-associated virus Rep. *Mol. Cell* 10, 327–337.
- Jones, T.A., Zou, J.Y., Cowan, S.W., and Kjeldgaard, M. (1991). Improved methods for building protein models in electron density maps and the location of errors in these models. *Acta Crystallogr. A* 47, 110–119.
- Kapitonov, V.V., and Jurka, J. (2001). Rolling-circle transposons in eukaryotes. *Proc. Natl. Acad. Sci. USA* 98, 8714–8719.
- Karberg, M., Guo, H., Zhong, J., Coon, R., Perutka, J., and Lambowitz, A.M. (2001). Group II introns as controllable gene targeting vectors for genetic manipulation of bacteria. *Nat. Biotechnol.* 19, 1162–1167.
- Kersulyte, D., Velapatino, B., Dailide, G., Mukhopadhyay, A.K., Ito, Y., Cahuayme, L., Parkinson, A.J., Gilman, R.H., and Berg, D.E. (2002). Transposable element ISHp608 of *Helicobacter pylori*: nonrandom geographic distribution, functional organization, and insertion specificity. *J. Bacteriol.* 184, 992–1002.
- Koonin, E.V., and Ilyina, T.V. (1993). Computer-assisted dissection of rolling circle DNA replication. *Biosystems* 30, 241–268.
- Lander, E.S., Linton, L.M., Birren, B., Nusbaum, C., Zody, M.C., Baldwin, J., Devon, K., Dewar, K., Doyle, M., FitzHugh, W., et al. (2001). Initial sequencing and analysis of the human genome. *Nature* 409, 860–921.
- Lambowitz, A.M., and Zimmerly, S. (2004). Mobile Group II Introns. *Annu. Rev. Genet.* 38, 1–35.
- Larkin, C., Datta, S., Harley, M.J., Anderson, B.J., Ebie, A., Hargreaves, V., and Schildbach, J.F. (2005). Inter- and intramolecular determinants of the specificity of single-stranded DNA binding and cleavage by the F factor relaxase. *Structure* 13, 1533–1544.

- Lee, H.H., Yoon, J.Y., Kim, H.S., Kang, J.Y., Kim, K.H., Kim, D.J., Ha, J.Y., Mikami, B., Yoon, H.J., and Suh, S.W. (2006). Crystal structure of a metal ion-bound IS200 transposase. *J. Biol. Chem.* *281*, 4261–4266.
- Mahillon, J., and Chandler, M. (1998). Insertion sequences. *Microbiol. Mol. Biol. Rev.* *62*, 725–774.
- Mennecier, S., Servant, P., Coste, G., Bailone, A., and Sommer, S. (2006). Mutagenesis via IS transposition in *Deinococcus radiodurans*. *Mol. Microbiol.* *59*, 317–325.
- Miskey, C., Izsvák, Z., Kawakami, K., and Ivics, Z. (2005). DNA transposons in vertebrate functional genomics. *Cell. Mol. Life Sci.* *62*, 629–641.
- Navaza, J. (2001). Implementation of molecular replacement in AMoRe. *Acta Crystallogr. D57*, 1367–1372.
- Noller, H.F. (2005). Reading the ribosome. *Science* *309*, 1508–1514.
- Otwinowski, Z., and Minor, W. (1997). Processing of X-ray Diffraction Data Collected in Oscillation Mode, Volume 276, Part A (New York: Academic Press).
- Ronning, D.R., Guynet, C., Ton-Hoang, B., Perez, Z.N., Ghirlando, R., Chandler, M., and Dyda, F. (2005). Active site sharing and subterminal hairpin recognition in a new class of DNA transposases. *Mol. Cell* *20*, 143–154.
- Schumacher, M.A., Karamooz, E., Zíková, A., Trantírek, L., and Lukes, J. (2006). Crystal structures of *T. brucei* MRP1/MRP2 guide-RNA binding complex reveal RNA matchmaking mechanism. *Cell* *126*, 701–711.
- Stokes, H.W., O’Gorman, D.B., Recchia, G.D., Parsekhian, M., and Hall, R.M. (1997). Structure and function of 59-base element recombination sites associated with mobile gene cassettes. *Mol. Microbiol.* *26*, 731–745.
- Toleman, M.A., Bennett, P.M., and Walsh, T.R. (2006). ISCR elements: Novel gene-capturing systems of the 21st century? *Microbiol. Mol. Biol. Rev.* *70*, 296–316.
- Ton-Hoang, B., Guynet, C., Ronning, D.R., Cointin-Marty, B., Dyda, F., and Chandler, M. (2005). Transposition of ISHp608, member of an unusual family of bacterial insertion sequences. *EMBO J.* *24*, 3325–3338.
- Zahradka, K., Slade, D., Bailone, A., Sommer, S., Aeverbeck, D., Petranovic, M., Lindner, A.B., and Radman, M. (2006). Reassembly of shattered chromosomes in *Deinococcus radiodurans*. *Nature* *443*, 569–573.

Accession Numbers

Coordinates have been deposited in the Protein Data Bank with the accession codes 2vih (TnpA/LE26), 2vic (TnpA/LE26+Mn²⁺), 2vhg (TnpA/RE31), 2vju (TnpA/RE35), and 2vjv (TnpA/LE26/D6).